NIH Public Access
Author Manuscript
Stem Cells. Author manuscript; available in PMC 2009 March 1.

Published in final edited form as:
Stem Cells. 2008 March ; 26(3): 600–610.

Characterization of Adult Prostatic Progenitor/Stem Cells Exhibiting Self-Renewal and Multilineage Differentiation

Wendy W. Barclay[a], **Linara S. Axanova**[a], **Wenhong Chen**[a], **Lina Romero**[a], **Sophia L. Maund**[a], **Shay Soker**[b], **Cynthia J. Lees**[c], and **Scott D. Cramer**[a]

a*Department of Cancer Biology, Wake Forest University School of Medicine, Winston-Salem, North Carolina, USA*

b*Institute for Regenerative Medicine, Wake Forest University School of Medicine, Winston-Salem, North Carolina, USA*

c*Department of Pathology, Wake Forest University School of Medicine, Winston-Salem, North Carolina, USA*

Abstract

Demonstration of the hallmarks of stem cells, self-renewal and multilineage differentiation, is a challenge that has not been met for numerous tissues postulated to possess adult stem cells, including prostate tissue. Using a defined medium, we reproducibly isolated and maintained adult mouse prostatic cells with characteristics of progenitor/stem cells. Clonal populations of cells demonstrated tissue-specific multilineage differentiation by their ability to generate organized prostatic ductal structures in vivo, with luminal and basal cell layers, when grafted under the renal capsules of mice in the presence of fetal rat urogenital mesenchyme. Complete differentiation was demonstrated by the expression and secretion of terminally differentiated prostatic secretory products into the lumens. Self-renewal was demonstrated by serial transplantation of clonal populations that generated fully differentiated ductal structures in vivo. In vitro, undifferentiated cells expressed markers associated with prostate stem cells, including Sca 1 and CD49f, as well as basal cell markers (p63 and cytokeratins 5 and 14) and, at a low level, luminal cell markers (androgen receptor and cytokeratins 8 and 18). When grafted and allowed to differentiate in the presence of fetal urogenital mesenchyme, the cells differentiated into luminal cells and basal cells with more restricted protein expression patterns. These studies are the first to report a reproducible system to assess adult prostatic progenitor/stem cells.

Keywords

Adult stem cells; Cell culture; Clonal assays; Self-renewal

INTRODUCTION

The adult prostate is a complex structure of branching epithelial ducts within a stromal matrix. The prostatic epithelium consists of two major epithelial cell types: a layer of columnar secretory cells surrounding the lumen and a layer of flattened cells adjacent to the basement membrane separating the luminal cells from the surrounding stroma [1]. Basal epithelial cells are androgen-independent, undifferentiated cells with high proliferative capacity and a low

Correspondence: Scott D. Cramer, Ph.D., Department of Cancer Biology, Medical Center Boulevard, Winston-Salem, North Carolina 27157, USA. Telephone: 336-713-7651; Fax: 336-713-7661; e-mail: scramer@wfubmc.edu.

DISCLOSURE OF POTENTIAL CONFLICTS OF INTEREST
The authors indicate no potential conflicts of interest.

NIH-PA Author Manuscript
NIH-PA Author Manuscript
NIH-PA Author Manuscript

NIH-PA Author Manuscript

NIH-PA Author Manuscript

NIH-PA Author Manuscript

apoptotic index. These cells are characterized by their expression of cytokeratins 5, 14, and 15, as well as p63 and the antiapoptotic protein bcl-2 [2,3]. Although basal cells are androgen-independent, a recent evaluation of markers in the murine prostate has also demonstrated expression of androgen receptor in basal cells [4]. Luminal epithelial cells are more differentiated, androgen-dependent cells with low proliferative capacity and high apoptotic index. These cells express androgen receptor (AR), cytokeratins 8 and 18 [5,6], and prostatic secretory products.

The modern version of the original prostate stem cell model [7] posits that there is a discrete population of undifferentiated cells, perhaps in a specialized niche that is located within the basal layer, that has the ability to differentiate into both basal and luminal cells [8-10]. The stem cells of the murine prostate express markers of basal cells, such as cytokeratin (CK) 5, p63, and CD49f (α6 integrin) [4,9], and possibly markers unique to the stem cell population, such as stem cell antigen 1 (Sca 1) [4,8-10]. In the human prostate, the stem cell is characterized by basal markers, such as CK5 and CK14, as well as positive expression of CD133 and α2/β1 integrin [11-13]. Cell division of a stem cell can produce one daughter cell that undergoes differentiation through a transit-amplifying population and one daughter cell that remains a stem cell (self-renewal).

The hallmarks of postnatal stem cells are the ability to self-renew and the ability to differentiate into mature progeny cells [14]. Evidence supports the concept of adult tissue-specific stem cells. These multipotent stem cells are thought to act as a reservoir for tissue regeneration after normal cellular turnover or in some tissues after injury or trauma. There is evidence for adult stem cells in numerous tissues, including the bone marrow [15-17], skin (hair follicle) [18], muscle [19], gastrointestinal tract [20], lung [21], heart [22], neural crest [23], breast [24,25], and prostate [8-10]. Studies in the prostate have used mixed populations of cells prospectively isolated for cell surface markers, such as Sca 1 and CD49f for the murine prostate [8-10] or CD44, CD133, and α2/β1 integrin for the human prostate [13,26], to generate ductal structures, supporting the presence of a progenitor/stem cell in the prostate. Multilineage differentiation from a single prostatic cell or a clonally derived cell population has not been demonstrated. Self-renewal of prostate progenitor cells has not been addressed rigorously.

MATERIALS AND METHODS

Culture of Mouse Prostatic Epithelial Cells

Adult mouse prostatic epithelial cells were isolated and maintained based on our previously described protocol [27]. A detailed protocol is available upon request. Briefly, anterior prostate lobes of 10-20 mice were pooled and finely minced with a sterile razor blade. Minced tissue was digested in 300 U/ml of type IV collagenase (Sigma-Aldrich, St. Louis, http://www.sigmaaldrich.com) in complete medium for approximately 60 minutes. Complete medium consisted of 50:50 Dulbecco's modified Eagle's medium (DMEM)/Ham's F-12 medium (F12) supplemented with 10 mg/ml fraction V bovine serum albumin (Sigma-Aldrich), 1% fetal bovine serum, cholera toxin (10 ng/ml; List Biologicals, Campbell, CA, http://www.listlabs.com), epidermal growth factor (10 ng/ml; BD Biosciences, San Jose, CA, http://www.bdbiosciences.com), bovine pituitary extract (28 μg/ml; Hammond Cell Tech, Windsor, CA, http://www.hammondcelltech.com), gentamicin (80 mg/ml; Sigma-Aldrich), insulin (8 μg/ml; Calbiochem, La Jolla, CA, http://www.emdbiosciences.com), α-tocopherol (2.3×10^6 M), transferrin (5 μg/ml; Sigma-Aldrich), and trace elements (final concentrations in medium: 1 nM $MnCl_2$, 500 nM Na_2SiO_3, 1 nM $(NH_4)_6Mo_7O_{24}$, 5 nM NH_4VO_3, 500 pM $NiCl_2$, 50 pM $SnCl_2$, 20 nM H_2SeO_3). Digestion was completed with 1 U/ml pronase (Sigma-Aldrich) for an additional 20 minutes. Digested organoids were separated from surrounding stromal debris on a Percoll density gradient. The isolated organoids were plated in complete growth medium on rat tail collagen-coated dishes, and medium was changed every other day.

NIH-PA Author Manuscript

NIH-PA Author Manuscript

NIH-PA Author Manuscript

Cells were passaged when 70%-80% confluent. After five or six passages, the cells were transferred to uncoated tissue culture dishes for routine growth. Cultured WFU3 mouse prostatic epithelial cells (MPECs) were used for grafting between passage 20 and passage 30. Cultured $Rb^{loxP/loxP}$ MPECs were used for grafting at passage 55 or 56.

Viral Infection

Ecotropic pBabe-puro-YFP retroviral production was performed using Ecopak cells (Clontech, Mountain View, CA, http://www.clontech.com) and the manufacturer's suggested protocols. Stable virus-producing Ecopak cells were selected by inclusion of 1 μg/ml puromycin in the medium. Ten ml of conditioned medium (without puromycin) from a confluent 10-cm puromycin-resistant Ecopak dish was passed through a 0.45-mm filter, and polybrene was added to an 8 μM final concentration. A semiconfluent 60-mm dish of WFU3 cells, passage 21, was incubated with 7 ml of filtered conditioned medium. After 8 hours, the conditioned medium was replaced with fresh complete growth medium. This infection was repeated once on the following day. Twenty-four hours after the second infection, the cells were switched to puromycin selection medium (complete growth medium with 1 μM puromycin). Cells were maintained in puromycin selection after this point. Individual clones were isolated by limiting dilution of passage 24 cells and expanded from 96-well plates to larger dishes prior to freezing aliquots.

Antibodies

Indirect immunofluorescence microscopy, immunohistochemistry, and immunoblots were performed as described below using antibodies to luminal-specific cytokeratin 8 (LE61) and basal-specific cytokeratin 14 (LL001) (antibodies were kindly provided by E. Birgette Lane [University of Scotland, Dundee, U.K.]), p63 (Santa Cruz Biotechnology Inc., Santa Cruz, CA, http://www.scbt.com), AR (N-20; Santa Cruz Biotechnology), and mouse dorsolateral secretory protein (mDLP) (kindly provided by G. Cunha [University of California at San Francisco]) [28]. Manufacturer-suggested dilutions were used for all primary antibodies. For indirect immunofluorescence experiments, secondary antibodies recognizing primary antibody host with either tetramethylrhodamine B isothiocyanate or fluorescein isothiocyanate (FITC) conjugates were used (Jackson Immunoresearch Laboratories, West Grove, PA, http://www.jacksonimmuno.com) at the recommended dilutions. For immunohistochemistry experiments, secondary antibodies with a horseradish peroxidase conjugate (Jackson Immunoresearch Laboratories) were used, and diaminobenzidine (DAB; Sigma-Aldrich) was used as the substrate.

Clonogenic Growth

Semiconfluent dishes of the indicated cells were lightly trypsinized with 0.2% trypsin/0.02% EDTA. The trypsin was inactivated by addition of two volumes of 0.1% trypsin inhibitor. The trypsinized cells were collected in Hepes-buffered saline, sedimented in a clinical centrifuge, and resuspended in an appropriate volume of complete growth medium. An aliquot was removed for counting using trypan blue exclusion to estimate viable cell number on a hemacytometer. Viable cells were inoculated on 60-mm dishes at the indicated numbers and allowed to grow until colonies contained approximately 50-100 cells on average (4-5 days). Cultures were terminated by fixation in 10% formalin and stained with a 0.1% crystal violet/95% ethanol solution for 10 minutes followed by rinsing with deionized water. Colonies were counted manually. Images were taken with a 4.0 megapixel Olympus CAMEDIA C-4000 zoom digital camera (Olympus, Center Valley, PA, http://www.olympusamerica.com). Statistical comparisons between groups was performed with analysis of variance followed by Sheffe's F-test using the statistical software package NCSS 6.0.22 (NCSS, Kaysville, UT, http://www.ncss.com).

NIH-PA Author Manuscript

NIH-PA Author Manuscript

NIH-PA Author Manuscript

Epithelial/Mesenchymal Cell Recombination

Embryonic rat urogenital sinuses (UGS) were microdissected from day 18 rat embryos using a Nikon SMZ1500 dissecting microscope (Nikon, Tokyo, http://www.nikon.com) and collected in sterile saline. Dissected UGS tissue was stored in Medium 199 (Invitrogen, Carlsbad, CA, http://www.invitrogen.com) at 4°C overnight. Following this overnight incubation, all UGS were incubated in one well of a six-well dish with 2 ml of a trypsin solution (1% trypsin [Sigma-Aldrich] in 1 × Hanks' balanced saline solution [Invitrogen]) at 4°C for approximately 30 minutes with care taken not to overdigest. After the proper digestion time, 1 ml of trypsin inhibitor (Sigma-Aldrich) and a few drops of fetal bovine serum (FBS) were added to the well to stop the trypsin digestion activity. The epithelial tubes were microscopically removed from the opaque mesenchymal tissue using ultrafine forceps and the needle point of a 1-ml syringe. The mesenchymal tissue was incubated with a collagenase solution (200 U/ml type I collagenase [Sigma-Aldrich] in RPMI medium [Invitrogen] supplemented with 10% FBS [Invitrogen] and 1% penicillin/streptomycin [Invitrogen]) at 37° C/5% CO_2 for 20 minutes with rocking. Following this incubation, the cells were collected by centrifugation (1,300 rpm, 5 minutes) and washed with 5 ml of Medium 199. Cells were collected by centrifugation and resuspended in 1 ml of complete growth medium. The resulting single-mesenchymal cell suspension was counted on a hemacytometer. MPECs (passage 20 or greater) were harvested from 10-cm cell culture dishes by trypsin digest and collected by centrifugation (1,300 rpm, 5 minutes). Cells were resuspended in DMEM/F12 complete and counted on a hemacytometer.

Rat-tail collagen [29] was diluted with glacial acetic acid (3:1). This diluted collagen solution was neutralized to pH 7.4 with a neutralizing solution (1.8:1 10 × Waymouth's [Sigma-Aldrich] and 0.34 N NaOH) and kept on ice to slow the formation of the collagen gel. In standard experiments, 2.5×10^5 rat urogenital mesenchymal cells were mixed or recombined with 1×10^5 epithelial cells. Recombined cell mixtures were embedded in 30 μl of neutralized rat tail collagen and plated as buttons onto a 24-well culture dish After the collagen buttons polymerized, 1 ml of RPMI medium supplemented with 10% FBS, penicillin (50 I.U./ml), and streptomycin (50 μg/ml) was added to each well. These buttons were incubated at 37°C/5% CO_2 overnight. Negative control buttons were also prepared with mesenchymal cells alone or epithelial cells alone. All surgeries were performed in animal facilities using protocols approved by the Wake Forest University Animal Care and Use Committee as described previously [30].

Graft Harvest and Tissue Processing

Animals were euthanized according to an approved protocol, and their kidneys were harvested. Kidneys were photographed using a Nikon SMZ1500 microscope and camera, and images were prepared using vendor-supplied software. The portions of the kidneys containing the implanted recombined cells were fixed overnight in buffered formalin and then processed and embedded in paraffin by the Histopathology Laboratory at Wake Forest University School of Medicine. Five-micrometer sections were prepared from paraffin-embedded tissue blocks using a microtome. Representative sections were stained with hematoxylin and eosin (H&E) following standard procedures to visualize morphology. In addition, sections were stained with Hoechst dye 33258 (Sigma-Aldrich). Phase-contrast and fluorescent images were captured using a fluorescent Nikon Eclipse 50i microscope and a Nikon digital camera.

For reisolation of puromycin-resistant cells after in vivo growth, a single graft was harvested after 8 weeks in vivo, minced, digested in 300 U/ml collagenase, rinsed, and plated on a 35-mm culture dish. Puromycin was added to growth medium at 1 μg/ml. After initial outgrowth, individual clones were selected by limiting dilution as described above.

NIH-PA Author Manuscript

NIH-PA Author Manuscript

NIH-PA Author Manuscript

Fluorescence-Activated Cell Sorting Analysis

Cells were seeded at a density of 10^5 cells per 10-cm plate. At approximately 70%-80% confluence, cells were washed with 5 mM EDTA/phosphate-buffered saline (PBS) solution and trypsinized. Trypsin was neutralized by trypsin inhibitor, and cells were pelleted and resuspended in 2% FBS/PBS. After being run through a 40-μm nylon cell strainer (BD Falcon, San Jose, CA, http://www.bdbiosciences.com), cells were counted using trypan blue dye and aliquoted to have at least 200,000 cells per sample. Individual samples were centrifuged, and supernatant was aspirated. The cell pellet was resuspended in 80 μl of 2% FBS/PBS buffer and blocked by adding 20 μl of blocking reagent (Miltenyi Biotec, Auburn, CA, http://www.miltenyibiotec.com) for 5 minutes on ice. Primary antibodies were added (1:25 for the phycoerythrin-conjugated antibodies), and cells were incubated for 1 hour at 4°C in the dark. Antibodies used included the following: Sca 1-FITC (Miltenyi Biotec), CD90-PE (BD Pharmingen, San Diego, http://www.bdbiosciences.com/index_us.shtml), CD44-PE (BD Pharmingen), CD73-PE (BD Pharmingen), CD34-PE (Becton, Dickinson and Company, Franklin Lakes, NJ, http://www.bd.com), and CD49f (BD Pharmingen). Appropriate isotype controls were added to the control samples. Cells were centrifuged, supernatant was aspirated, and cells were washed twice with 2% FBS/PBS buffer. For CD49f antibody, a goat-PE secondary antibody was used for 30 minutes, 4°C, in the dark, which was followed by washing as described above. Cells were resuspended in 2% FBS/PBS buffer (300 μl) and kept on ice in the dark until ready to be evaluated by fluorescence-activated cell sorting (FACS). FACS analysis was performed with a FACSCalibur E6204 machine and vendor-provided software (CellQuest Pro version 5.1, BD Biosciences).

Immunohistochemistry

For immunohistochemical staining of proteins, sections were deparaffinized by successive incubation in xylene, 100% ethanol, and then 90% ethanol following standard procedures. The endogenous peroxidase activity was blocked by incubation for 20 minutes at room temperature in 0.5% H_2O_2 in water. Sections were washed three times in PBS. Retrieval of antigens was performed by incubating the sections in antigen retrieval solution (Sigma-Aldrich) for 1 hour in a 95°C water bath. After the sections were allowed to cool, samples were washed in PBS and blocked with 3% bovine serum albumin in PBS for 30 minutes at room temperature. After blocking, sections were incubated with primary antibody for 1 hour at room temperature and washed. Sections were then incubated with the appropriate secondary antibody with a peroxidase conjugate, washed, and then incubated with DAB for approximately 2-5 minutes. Following counterstain with hematoxylin (Sigma-Aldrich) and clearing of the sections through ethanol and xylene, coverslips were mounted using Permount medium.

Immunofluorescence and Immunoblotting

The procedures for immunoblotting of protein lysates and indirect immunofluorescence microscopy studies using cells grown in monolayer culture is described in detail elsewhere [27].

RESULTS

Stable Cultures of Adult Prostatic Cells with Tissue Regenerative Capacity

We previously published a protocol for the isolation of MPECs [27]. This system is highly reproducible and has been used to isolate mouse prostatic cells from numerous genetic backgrounds. During the characterization of these cells, we previously discovered several unique features suggesting that they have progenitor/stem cell characteristics, such as the ability to form spheroids in vitro and growth in three-dimensional collagen gels [27]. To address the question of whether MPECs isolated by our protocol possess the ability to differentiate into

NIH-PA Author Manuscript

NIH-PA Author Manuscript

NIH-PA Author Manuscript

luminal and basal cells, we used a modification of the Cunha prostate recombination model [31-36]. A schematic of our protocol is depicted in Figure 1A. Isolated prostatic epithelial cells were recombined with fetal rat urogenital mesenchyme (rUGM) and implanted under the renal capsule of a nude mouse. Ductal formation from progenitor cells is controlled by the inductive effects of the embryonic mesenchyme [31-36]. In this initial experiment, a mixed population of MPECs (WFU3, described in [27]) were grafted with rUGM cells ($n = 5$ grafts). As a positive control, microdissected mouse prostatic epithelial ducts (mPEDs) from 12-week old B1/6;129 SVEV males recombined with rUGM were used ($n = 5$ grafts). As a negative control, rUGM cells alone were used ($n = 2$ grafts). Animals were euthanized 3 months after engraftment. rUGM alone grafts showed no evidence of growth on gross examination (Fig. 1A, inset). However, grafts containing ductal pieces (Fig. 1A, inset, mPED) or MPECs (Fig. 1A, inset, MPEC) showed growth of cystic-looking structures (Fig. 1A, inset, arrows) on gross examination. Histological examination of sections from formalin-fixed, paraffin-embedded samples demonstrated that MPEC grafts generated luminal structures indistinguishable from those of grafts generated from ducts (Fig. 1B). To control for potential contamination of rUGM with rat epithelium, sections were stained with Hoechst dye and visualized by fluorescence microscopy. Hoechst dye specifically stains mouse nuclei with a punctate pattern that is not observed in rat cells. Our results confirm that the ductal structures were of mouse origin (Fig. 1C, arrows), whereas the majority of cells in the surrounding stroma were of rat origin (Fig. 1C, arrowheads). Basal cells in MPEC grafts were observed by immunohistochemical detection to express p63 and cytokeratin 14 (Fig. 2A, 2B, arrows), whereas luminal cells lacked expression of these two markers (Fig. 2A, 2B, arrowheads). Cytokeratin 8/18 expression was specifically found in the luminal cells (Fig. 2C). Complete differentiation of ductal structures was demonstrated by the presence of immunoreactivity to anti-mouse dorsolateral prostatic secretory protein in the lumens (Fig. 2D, mDLP).

Clonal MPECs Undergo Multilineage Differentiation

To evaluate whether our mixed population of WFU3 prostatic epithelial cells contained a common progenitor cell for both luminal and basal epithelial cells of the prostate, we isolated clonal populations of cells by limiting dilution and grafted randomly selected clonal populations under the renal capsules of nude mice (Fig. 3A). Two of three clones tested (clones 1 and 3) generated ductal structures at 10 weeks postengraftment, as determined by histological assessment of fixed sections (Fig. 3B). A third clone generated no discernable differentiation (Fig. 3B, clone 6). Grafting of epithelial cells in the absence of mesenchyme produced no discernable growth (data not shown). Clone 3 was further evaluated for expression of luminal and basal cell markers. Here, we used AR expression as a marker for luminal cells and p63 expression for basal cells. These two markers were chosen because of their high specificity and their nuclear localization. AR was found localized predominantly in the luminal cell nuclei and in mesenchymal cells, whereas p63 labeling was specifically in basal cell nuclei (Fig. 3C). Functional differentiation of luminal cells into secretory epithelium was detected by the presence of mDLP in the lumens (Fig. 3C). We repeated these studies with two independent clonal populations of cells derived from adult mice of a different genetic background ($RB^{loxP/LoxP}$) [27]. Tissue recombinants with rUGM generated ductal-like structures (Fig. 4A), and the cells differentiated into luminal and basal cells (Fig. 4B), demonstrating the reproducibility of this system. To our knowledge, these results are the first to clearly demonstrate that a clonal population of cells derived from the adult prostate possesses the ability for multilineage differentiation. These data support the hypothesis that a common progenitor cell generates both luminal and basal cell types within the prostate.

Adult Prostate Progenitor Cells Undergo Self-Renewal In Vivo

Our clonal adult prostatic cells represent a common progenitor population for both luminal and basal cells. These cells may represent a stem/progenitor cell with the ability for self-renewal.

NIH-PA Author Manuscript

NIH-PA Author Manuscript

NIH-PA Author Manuscript

Alternatively, they may represent a transit-amplifying population that has more limited replicative capacity and that lacks the ability for self-renewal. Prior to the clonal isolation described above, MPEC mixed cells were rendered puromycin-resistant by infection with pBabe-Puro retroviral vector (schema depicted in Fig. 5A). Clonal MPECs (Fig. 3, clone 3) were grafted with rUGM and allowed to grow for 8 weeks in vivo. Cells were isolated from a single graft by mincing and plating in medium that contained puromycin. Clones of puromycin-resistant cells were isolated by limiting dilution, expanded, and subsequently grafted with rUGM. This experiment was performed (repeated) on cells isolated from two separate individual grafts. Expanded clones were regrafted with rUGM under the renal capsules of nude mice and allowed to grow for 8 weeks. Figure 5B shows that rUGM alone formed no growth. SRB2, a clone derived from the graft shown in Figure 5A exhibited robust growth in both grafts (Fig. 5B). SR28, a clone that was generated from a separate graft that is not depicted, also showed similar robust growth (Fig. 5B). Epithelial cells grafted alone produced no graft (data not shown). Histological examination of fixed sections demonstrated organized luminal structures. Immunohistochemical detection of basal cell differentiation (p63) and luminal cell differentiation (AR), were consistent with differentiation of both clones into both basal and luminal cells (Fig. 5C). In addition, the luminal cells made mDLP and secreted mDLP into the lumens (Fig. 5C). These results confirm the long-term retention of a progenitor cell in vivo and suggest that they retain the ability for self-renewal.

Marker Expression in Prostatic Stem/Progenitor Cells

We next performed clonogenic assays to assess the colony-forming ability of the cells as an estimate of the number of cells with self-renewal potential within the cultured populations. We assessed the clonal efficiency (judged by the number of cells inoculated vs. the number of colonies that arose) of the mixed-population WFU3 cells, a clonal derivative of WFU3 (WFU3 clone 3 cells), and a mixed population derived from a graft of WFU3 clone 3 (serial recombinant [SR] parent cells). Figure 6A shows representative dishes from clonogenic assays and a graphical representation of the mean data from quadruplicate dishes. WFU3 and SR parental cells had similar clonogenic growth (35% and 29% efficiency, respectively). In contrast, WFU3 clone 3 cells had nearly double the efficiency, with 66% of cells generating colonies. The number of colonies generated by WFU3 clone 3 cells was statistically significantly different from the number of colonies generated by mixed populations of WFU3 or SR parent cells at all of the inoculation densities.

These data implied that clonal selection of cells enriches for cells with stem cell-like properties. Previous studies have suggested that the putative prostate progenitor/stem cell is located in the basal layer and may express markers of basal cells. We next compared in vitro expression patterns of markers that distinguish between basal and luminal cells in WFU3, WFU3 clone 3, and SR parent cells. For these studies, we used CK8 and AR as markers of luminal cells and CK14 and p63 as markers of basal cells. In vitro, all three cell lines were found to express markers associated with both basal cells (Fig. 6B, CK14 and p63) and luminal cells (Fig. 6B, CK8 and AR), although there was heterogeneous expression within a population, suggesting partial differentiation within the culture conditions. The data were confirmed in the $Rb^{loxP/LoxP}$ cells (Fig. 4C). Although these data were not quantitative, by visual inspection the WFU3 clone 3 cells appeared to strongly express basal cell markers (p63 and CK14) in a greater proportion of cells than either of the unselected cell populations (WFU3 or SR parent). This supported the possibility that the progenitor/stem cell population represents a finite population in the cultures, with other cells representing in vitro-differentiated progeny. To further assess relative p63 and AR expression in the different populations, we also performed immunoblot analysis with cell lysates from semiconfluent cultures, probing for p63, AR, and β-actin expression. Figure 6C shows that after normalization to β-actin expression, WFU3 clone 3 cells had a greatly reduced expression of AR relative to either WFU3 or SR parent cells. The ratio

NIH-PA Author Manuscript

NIH-PA Author Manuscript

NIH-PA Author Manuscript

of p63 to AR expression went from 1.4 or 1.08 for WFU3 or SR parent cells, respectively, to 3 for WFU3 clone 3 cells. The clonogenic data that demonstrate increased clonogenicity of the WFU3 clone 3 cells, together with the increased ratio of p63 to AR in these same cells, support a model in which the prostate progenitor/stem cell expresses high p63 and low AR.

Prostate Progenitor Stem Cells Express Sca 1 and CD49f

Recent data have demonstrated enrichment of mouse prostate progenitor stem cells using cell surface expression of Sca 1 and CD49f along with exclusion of CD34 (stromal lineage)-expressing cells [9]. We assessed a panel of cell surface markers using FACS analysis on WFU3 cells (Fig. 7A). WFU3 cells were found to be negative for CD34, CD44, CD73, and CD90 expression, relative to isotype control. In contrast, 99% of WFU3 cells were found to be positive for Sca 1 expression and CD49f. This assay was repeated twice with similar results. We next compared the expression patterns of these surface markers on WFU3, WFU3 clone 3, and SR parent cells. All three cell populations had similar low to absent expression of CD34, CD44, CD73, and CD90 (Fig. 7B). CD49f was expressed in 99% of cells in all three populations, with a similar median intensity of expression. Sca 1 expression was present in all three populations. Both WFU3 and WFU3 clone 3 cells expressed Sca 1 in 99% of cells, although clone 3 cells had an approximately 25% increase in the median intensity of Sca 1 expression over WFU3 cells. In contrast, the SR parent expressed Sca 1 at a lower median intensity (approximately 40% of WFU3 cells), and fewer cells were scored positive (81.5%).

DISCUSSION

We conclude that the MPEC culture system that we developed isolates and maintains adult mouse prostatic progenitor/stem cells. Clonal populations of these cells given appropriate differentiation signals in vivo undergo multilineage differentiation, and serial grafting demonstrates that this ability is retained long-term, supporting self-renewal. In vitro, these cells express markers normally associated with both prostatic basal cells (p63, and CK14) and prostatic luminal cells (AR, CK8, and CK18). We have tested these markers in MPECs isolated from six different genetic backgrounds with virtually identical results ([27]; W.W. Barclay and S.D. Cramer, unpublished data), highlighting the reproducibility of this system. The cells undergo tissue-specific multilineage differentiation to form fully differentiated basal cells and fully differentiated luminal cells with secretion of prostatic secretory proteins into the lumen. These studies are important because they support and extend the work of others that indicate that there is a progenitor/stem cell population in the adult prostate [8,10]. Perhaps more importantly, these studies describe a system with great utility for the further characterization of adult prostatic progenitor/stem cells. Definitive work on this population of cells has been hampered by a lack of reproducible model systems. Potential uses of the system described here are the identification of unique markers for the prostate progenitor/stem cell, understanding the developmental biology of prostate differentiation pathways, and understanding the stem cell properties of prostate cancer cells.

In this report, we show through studies with clonally derived populations of cells the ability of the prostate progenitor/stem cell to undergo prostate tissue-specific multilineage differentiation. Although others have used cells sorted on the basis of surface marker expression to enrich for putative progenitor/stem cells for generation of differentiated prostatic ductal structures [8-10], this work is the first to use a clonally derived population for such studies. Our development of an appropriate method for the growth of prostate progenitor/stem cells has made these studies possible.

We present data on luminal and basal cell markers from mixed populations of cells versus a clonal population of cells with enriched stem cell characteristics, such as clonogenic growth. Our data support a model that includes high p63 and low AR expression. The p53 homolog

NIH-PA Author Manuscript

NIH-PA Author Manuscript

NIH-PA Author Manuscript

p63 has a controversial role in prostatic progenitor/stem cells. p63 is expressed in basal cells of the prostate [37], and Signoretti et al. demonstrated that p63-/- mice do not form a prostate [38]. These data imply a pivotal role for p63 in prostate development. However, Kurita et al. rescued embryonic prostatic epithelium from p63-/- mice and demonstrated that when this epithelium is transplanted with rUGM, the cells differentiate into secretory epithelium [39]. Basal cells are absent. These data suggested that the prostatic secretory epithelial cell can be generated from a p63-/- cell. More recently, Signoretti et al. used p63-/- embryo injected with p63+/+ β-galactosidase-positive embryonic stem cells [3]. Using β-galactosidase staining, they demonstrated that 100% of basal and luminal epithelial cells in the prostate were derived from the p63+/+ cells in these chimeras [3]. None of the prostatic cells were β-galactosidase-negative. This study went on to suggest that p63 is required for prostate lineage differentiation. In our study, we did not test the requirement of p63 for maintenance of the progenitor/stem cell phenotype of our MPECs. However, our observations that clonally derived cells that express p63 are progenitor/stem cells in the prostate support the conclusions of Signoretti et al. [3,38].

Several groups have used Sca 1 expression as a selective marker for enrichment of the prostate progenitor/stem cell from the mouse. Our data that demonstrate high Sca 1 expression in our cultured progenitor/stem cells is in agreement with that of previous studies. Interestingly, the clonally derived population of cells, WFU3 clone 3, exhibited the highest expression of Sca 1, supporting other data that suggest that this cell line has increased stem cell characteristics.

Self-renewal is a feature of adult progenitor/stem cells that has not been previously demonstrated for the prostate. We used serial transplantation (grafting) to assess long-term retention of a progenitor/stem cell population. Although this is not a perfect assay, it is generally considered the best currently available for study of self-renewal [40]. Our data demonstrate self-renewal by our ability to reisolate, clonally derive, and regraft cells with multilineage capabilities. We also rederived regrafted cells and found they retained the ability to form spheroids (data not shown). Some reports suggest that the ability to form spheroids in vitro is a characteristic of adult stem cells [41,42].

From these results, taken together, we conclude that the system that we have developed maintains a population of cells with the hallmark features of progenitor/stem cells: multilineage differentiation and self-renewal. Future use of this model should reveal information regarding prostate differentiation and possibly the origins of prostate cancer.

ACKNOWLEDGMENTS

We thank Jerry Cunha for providing training and encouragement in the prostate tissue recombination method and providing the mDLP antibody. We also thank Yun Kit (Don) Hom and Anne Donjacour for help with the renal grafting/tissue recombination methodology. We thank E. Birgette Lane for providing cytokeratin antibodies. This work was supported by grants R01-CA101023 and the Kulynych Interdisciplinary Cancer Research Fund (to S.D.C.). W.W.B. and S.L.M. were supported by a training grant (T32 CA079448) from the National Cancer Institute.

REFERENCES

1. Wang Y, Hayward S, Cao M, et al. Cell differentiation lineage in the prostate. Differentiation 2001;68:270–279. [PubMed: 11776479]
2. Magi-Galluzzi C, Loda M. Molecular events in the early phases of prostate carcinogenesis. Eur Urol 1996;30:167–176. [PubMed: 8875197]
3. Signoretti S, Pires M, Lindauer M, et al. p63 regulates commitment to the prostate cell lineage. Proc Natl Acad Sci USA 2005;102:11355–11360. [PubMed: 16051706]
4. Wang S, Garcia A, Wu M, et al. Pten deletion leads to the expansion of a prostatic stem/progenitor cell subpopulation and tumor initiation. Proc Natl Acad Sci U S A 2006;03:1480–1485. [PubMed: 16432235]

NIH-PA Author Manuscript

NIH-PA Author Manuscript

NIH-PA Author Manuscript

5. Aumuller G. Morphologic and endocrine aspects of prostatic function. Prostate 1983;4:195–214. [PubMed: 6340083]
6. Liu A, True D, LaTray L, et al. Cell-cell interaction in prostate gene regulation and cytodifferentiation. Proc Natl Acad Sci USA 1997;94:10705–10710. [PubMed: 9380699]
7. Isaacs, J. Control of cell proliferation and cell death in the normal and neoplastic prostate: A stem cell model. In: Rodgers, C.; Coffey, D.; Cunha, G., et al., editors. Benign Prostatic Hyperplasia. II. NIH; Bethesda, MD: 1987. p. 85-94.
8. Burger P, Xiong X, Coetzee S, et al. Sca-1 expression identifies stem cells in the proximal region of prostatic ducts with high capacity to reconstitute prostatic tissue. Proc Natl Acad Sci U S A 2005;102:7180–7185. [PubMed: 15899981]
9. Lawson D, Xon L, Lukacs R, et al. Isolation and functional characterization of murine prostate stem cells. Proc Natl Acad Sci U S A 2007;104:181–186. [PubMed: 17185413]
10. Xin L, Lawson D, Witte O. The Sca-1 cell surface marker enriches for a prostate-regenerating cell population that can initiate prostate tumorigenesis. Proc Natl Acad Sci U S A 2005;102:6242–6947.
11. Collins A, Habib F, Maitland N, et al. Identification and isolation of human prostate epithelial stem cells based on $\alpha 2\beta 1$-integrin expression. J Cell Sci 2001;114:3865–3872. [PubMed: 11719553]
12. Miki J, Furusato B, Li H, et al. Identification of putative stem cell markers, CD133 and CXCR4, in hTert-immortalized primary nonmalignant and malignant tumor-derived human prostate epithelial cell lines and in prostate cancer specimens. Cancer Res 2007;67:3153–3161. [PubMed: 17409422]
13. Richardson G, Robson C, Lang S, et al. CD133, a novel marker for human prostatic epithelial stem cells. J Cell Sci 2004;117:3539–3545. [PubMed: 15226377]
14. Reya T, Morrison S, Clarke M, et al. Stem cells, cancer, and cancer stem cells. Nature 2001;414:105–111. [PubMed: 11689955]
15. Baum C, Weissman I, Tsukamoto A, et al. Isolation of a candidate human hematopoietic stem-cell population. Proc Natl Acad Sci USA 1992;89:2804–2808. [PubMed: 1372992]
16. Morrison S, Weissman I. The long-term repopulating subset of hematopoietic stem cells is deterministic and isolatable by phenotype. Immunity 1994;1:661–673. [PubMed: 7541305]
17. Spangrude G, Heimfeld S, Wieissman I. Purification and characterization of mouse hematopoietic stem cells. Science 1988;241:58–62. [PubMed: 2898810]
18. Cotsarelis G, Sun T, Lavker R. Label-retaining cells reside in the bulge area of pilosebaceous unit: Implications for follicular stem cells, hair cycle, and skin carcinogenesis. Cell 1990;61:1329–1337. [PubMed: 2364430]
19. Seale P, Asakura A, Rudnicki M. The potential of muscle stem cells. Dev Cell 2001;1:333–342. [PubMed: 11702945]
20. Loeffler M, Birke A, Winton D, et al. Somatic mutation, monoclonality and stochastic models of stem cell organization of the intestinal crypt. J Theor Biol 1993;160:471–491. [PubMed: 8501919]
21. Kim C, Jackson E, Woolfenden A, et al. Identification of bronchioalveolar stem cells in normal lung and lung cancer. Cell 2005;212:823–835. [PubMed: 15960971]
22. Beltrami A, Barlucchi L, Torella D, et al. Adult cardiac stem cells are multipotent and support myocardial regeneration. Cell 2003;114:763–776. [PubMed: 14505575]
23. Doetsch F, Caille I, Lim D, et al. Subventricular zone astrocytes are neuronal stem cells in the adult mammalian brain. Cell 1999;97:703–716. [PubMed: 10380923]
24. Shackleton M, Vaillant F, Simpson K, et al. Generation of functional mammary gland from a single cell. Nature 2006;439:84–88. [PubMed: 16397499]
25. Smith G, Medina D. A morphologically distinct candidate for an epithelial stem cell in mouse mammary gland. J Cell Sci 1988;90:173–183. [PubMed: 3198708]
26. Collins A, Berry P, Hyde C, et al. Prospective identification of tumorigenic prostate cancer stem cells. Cancer Res 2005;65:10946–10951. [PubMed: 16322242]
27. Barclay W, Cramer S. Culture of mouse prostatic epithelial cells from genetically engineered mice. Prostate 2005;63:291–298. [PubMed: 15599944]
28. Donjacour A, Cunha G. Assessment of prostatic protein secretion in tissue recombinants made of urogenital sinus mesenchyme and urothelium from normal and androgen-insensitive mice. Endocrinology 1993;132:2342–2350. [PubMed: 7684975]

NIH-PA Author Manuscript

NIH-PA Author Manuscript

NIH-PA Author Manuscript

29. Richards J, Larson L, Yang J, et al. Method for culturing mammary epithelial cells in rat tail collagen matrix. J Tissue Cult Methods 1983;8:31–36.

30. Barclay W, Woodruff R, Hall M, et al. A system for studying epithelialstromal interactions reveals distinct inductive abilities of stromal cells from benign prostatic hyperplasia and prostate cancer. Endocrinology 2005;146:13–18. [PubMed: 15471963]

31. Cunha G. Epithelio-mesenchymal interaction in primordial gland structures which become responsive to androgenic stimulation. Anat Rec 1972;172:179–196. [PubMed: 5012433]

32. Cunha GR, Chung LW. Stromal-epithelial interactions-I. Induction of prostatic phenotype in urothelium of testicular feminized (Tfm/y) mice. J Steroid Biochem 1981;14:1317–1324. [PubMed: 6460136]

33. Cunha GR, Fujii H, Neubauer BL, et al. Epithelial-mesenchymal interactions in prostatic development. I. morphological observations of prostatic induction by urogenital sinus mesenchyme in epithelium of the adult rodent urinary bladder. J Cell Biol 1983;96:1662–1670. [PubMed: 6853597]

34. Cunha GR. Androgenic effects upon prostatic epithelium are mediated via trophic influences from stroma. Prog Clin Biol Res 1984;145:81–102. [PubMed: 6371832]

35. Cunha G, Donjacour A, Cooke P, et al. The endocrinology and developmental biology of the prostate. Endocr Rev 1987;8:338–362. [PubMed: 3308446]

36. Day K, McCabe M, Zhao X, et al. Rescue of embryonic epithelium reveals that the homozygous deletion of the retinoblastoma gene confers growth factor independence and immortality but does not influence epithelial differentiation of tissue morphogenesis. J Biol Chem 2002;277:44475–44484. [PubMed: 12191999]

37. Yang A, Kaghad M, Wang Y, et al. p63, a p53 homolog at 3q27-29, encodes multiple products with transactivating, death inducing, and dominant-negative activities. Mol Cell 1998;2:305–316. [PubMed: 9774969]

38. Signoretti S, Waltregny D, Dilks J, et al. p63 is a prostate basal cell marker and is required for prostate development. Am J Pathol 2000;157:1769–1775. [PubMed: 11106548]

39. Kurita T, Medina R, Mills A, et al. Role of p63 and basal cells in the prostate. Development 2004;131:4955–4964. [PubMed: 15371309]

40. Clarke M, Dick J, Dirks P, et al. Cancer stem cells-Perspectives on current status and future directions: AACR workshop on cancer stem cells. Cancer Res 2006;66:9339–9344. [PubMed: 16990346]

41. Dontu G, Abdallah W, Foley J, et al. In vitro propagation and transcriptional profiling of human mammary stem/progenitor cells. Genes Dev 2003;17:1253–1270. [PubMed: 12756227]

42. Dontu G, Wicha M. Survival of mammary stem cells in suspension culture: Implications for stem cell biology and neoplasia. J Mammary Gland Biol Neoplasia 2005;10:75–86. [PubMed: 15886888]

NIH-PA Author Manuscript
NIH-PA Author Manuscript
NIH-PA Author Manuscript

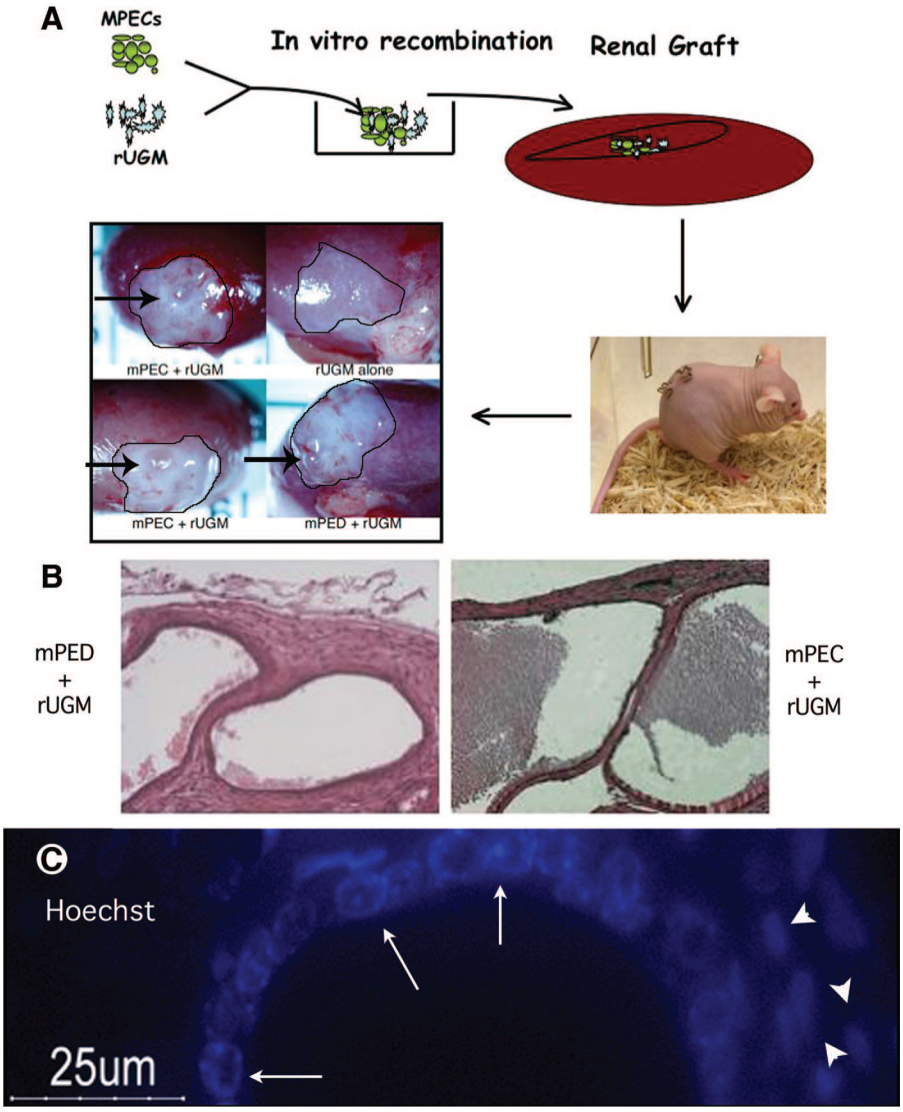

Figure 1.

Mixed-population MPECs generate luminal structures in vivo. **(A):** Schematic of the modified tissue recombination protocol. MPECs (100,000 cells) were mixed with microdissected day 18 fetal rUGM (250,000 cells) that had been cleared of fetal epithelium. The tissue recombinants were grafted under the renal capsules of nude mice and allowed to remain for various periods (3 months in this experiment). Controls were rUGM alone (negative control for rat epithelial contamination) and microdissected mPED + rUGM (positive control). **(B):** H&E staining of mPED + rUGM control (anterior ducts) and MPEC + rUGM. Original magnification, ×25. **(C):** Hoechst dye labeling identified punctate nuclear staining (arrows) indicative of the mouse origin of the ductal structures (note diffuse nuclear staining of adjacent rat mesenchymal cells, arrowheads). Abbreviations: MPEC, mouse prostatic epithelial cell; mPED, mouse prostatic epithelial duct; rUGM, rat urogenital mesenchyme; um, micrometer.

NIH-PA Author Manuscript
NIH-PA Author Manuscript
NIH-PA Author Manuscript

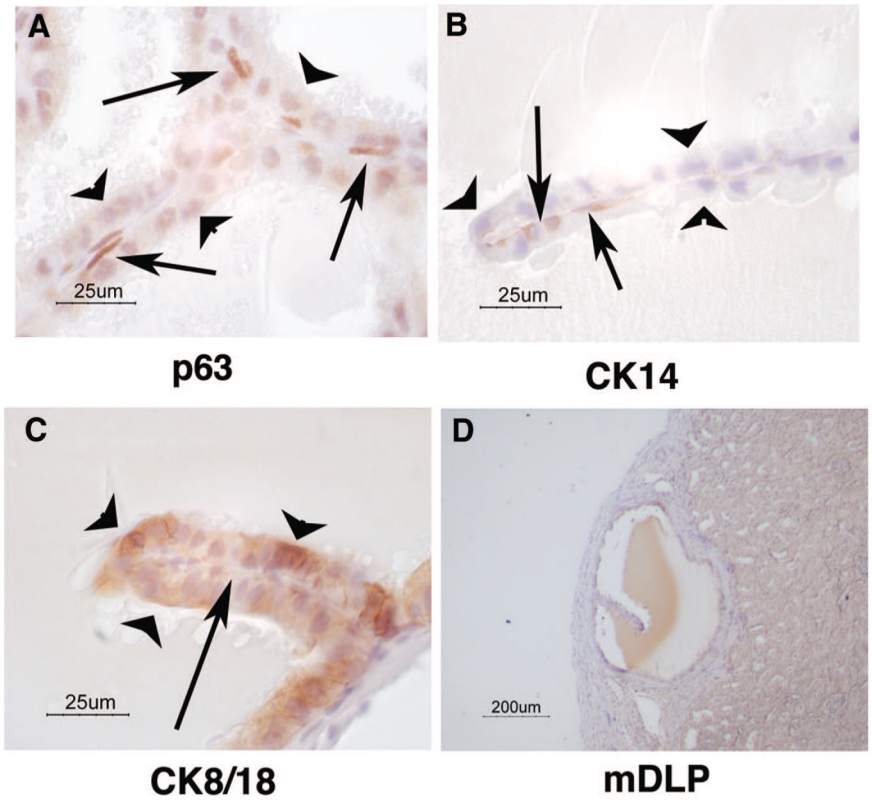

Figure 2.

Mouse prostatic epithelial cells differentiate into luminal and basal cells that make prostate secretory products. Sections were prepared from grafts depicted in Figure 1. Sections were probed with antibodies to lineage-specific markers p63 **(A)**, CK14 **(B)**, CK8/18 **(C)**, and mDLP **(D)**. Arrows point to basally located cells; arrowheads point to luminal cells. Abbreviations: CK, cytokeratin; mDLP, mouse dorsolateral secretory protein; um, micrometer.

NIH-PA Author Manuscript
NIH-PA Author Manuscript
NIH-PA Author Manuscript

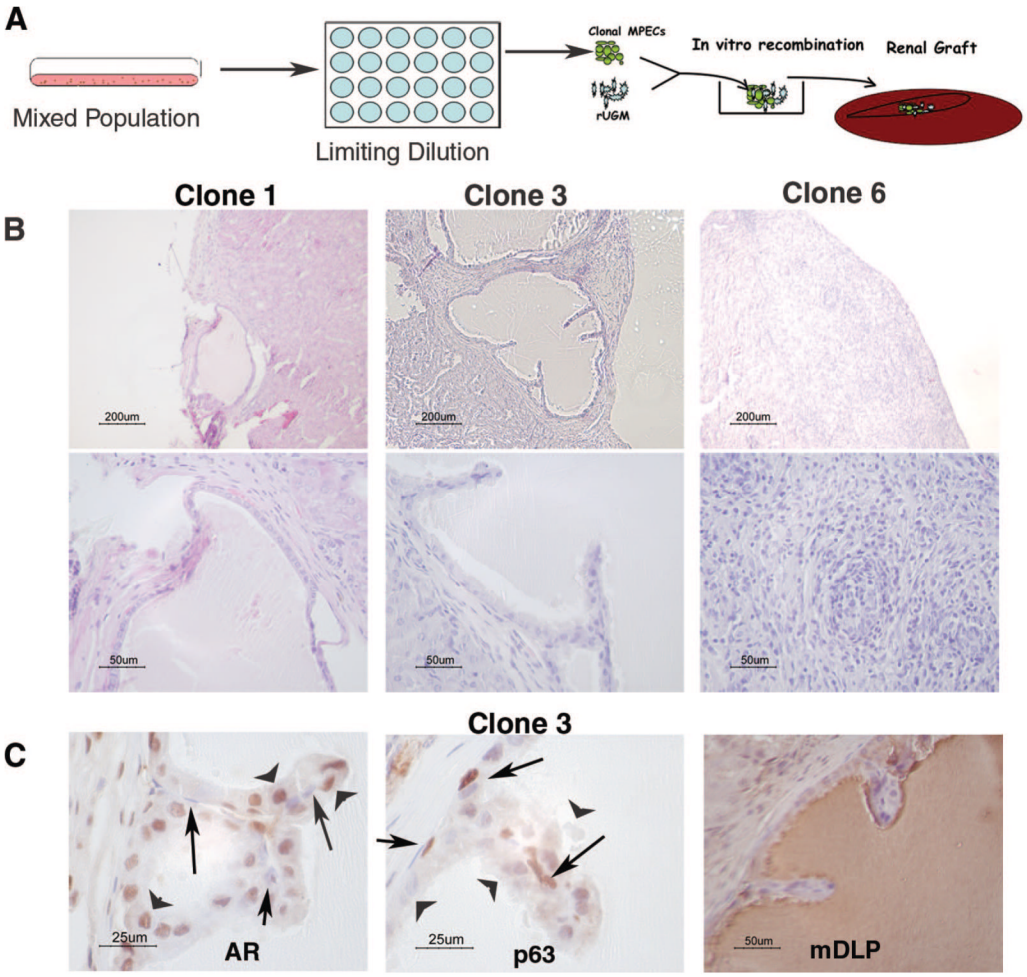

Figure 3.

Clonal populations of MPECs form ductal structures. **(A):** Schematic of experiment. A mixed population of WFU3 cells was inoculated on a 96-well culture dish at 1/2 cell per well. Individual colonies were expanded and grafted with rUGM. **(B):** H&E sections from grafts from three independent clones. Upper panels are low-magnification images of the slides. **(C):** Immunohistochemical staining of AR, p63, and mDLP of grafted WFU3 clone 3 cells. Arrows point to basal cells; arrowheads point to luminal cells. Abbreviations: AR, androgen receptor; mDLP, mouse dorsolateral secretory protein; MPEC, mouse prostatic epithelial cell; rUGM, rat urogenital mesenchyme; um, micrometer.

NIH-PA Author Manuscript

NIH-PA Author Manuscript

NIH-PA Author Manuscript

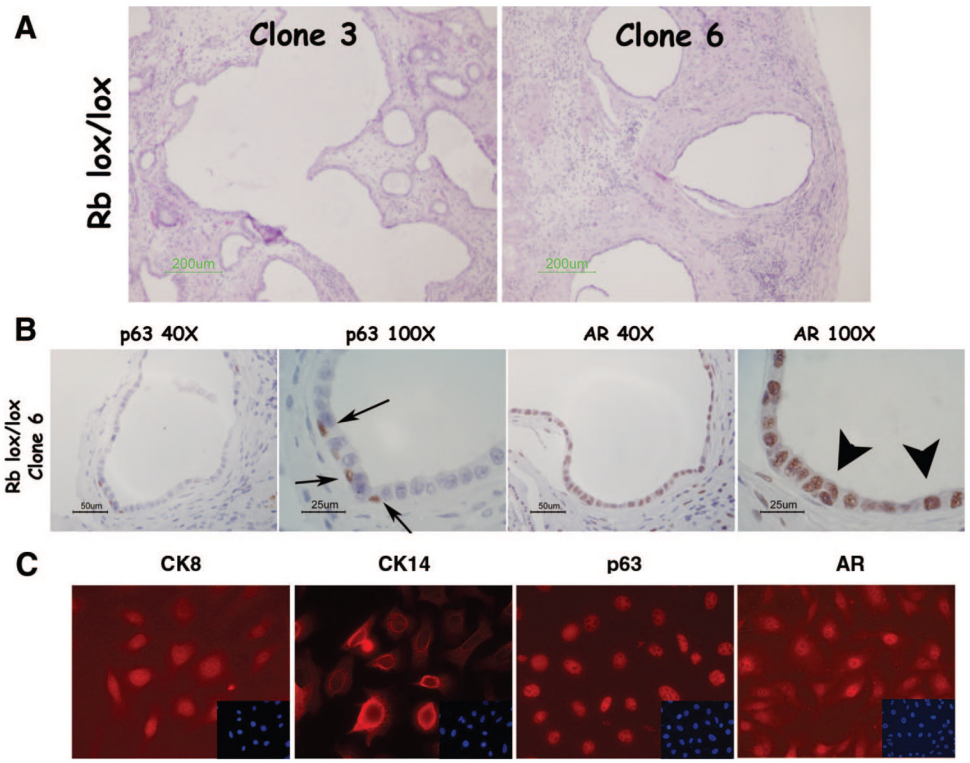

Figure 4.

Clonal $Rb^{loxP/LoxP}$ mouse prostatic epithelial cells (MPECs) undergo multilineage differentiation in vivo. MPECs were isolated from $Rb^{loxP/LoxP}$ animals as previously described [27]. The parental population was subjected to limiting dilution as described for WFU3 MPECs, and clones were grafted with rat urogenital mesenchyme in nude mice. **(A):** Histology of two independent clones shows luminal structures. **(B):** Immunodetection of p63 and AR shows a defined basal layer (arrows) and a defined luminal layer (arrowheads). **(C):** In vitro, the parental cells expressed luminal (CK8 and AR) and basal (CK14 and p63) markers. Insets show 4,6-diamidino-2-phenylindole stain. Original magnification, ×60. Abbreviations: AR, androgen receptor; CK, cytokeratin; um, micrometer.

NIH-PA Author Manuscript
NIH-PA Author Manuscript
NIH-PA Author Manuscript

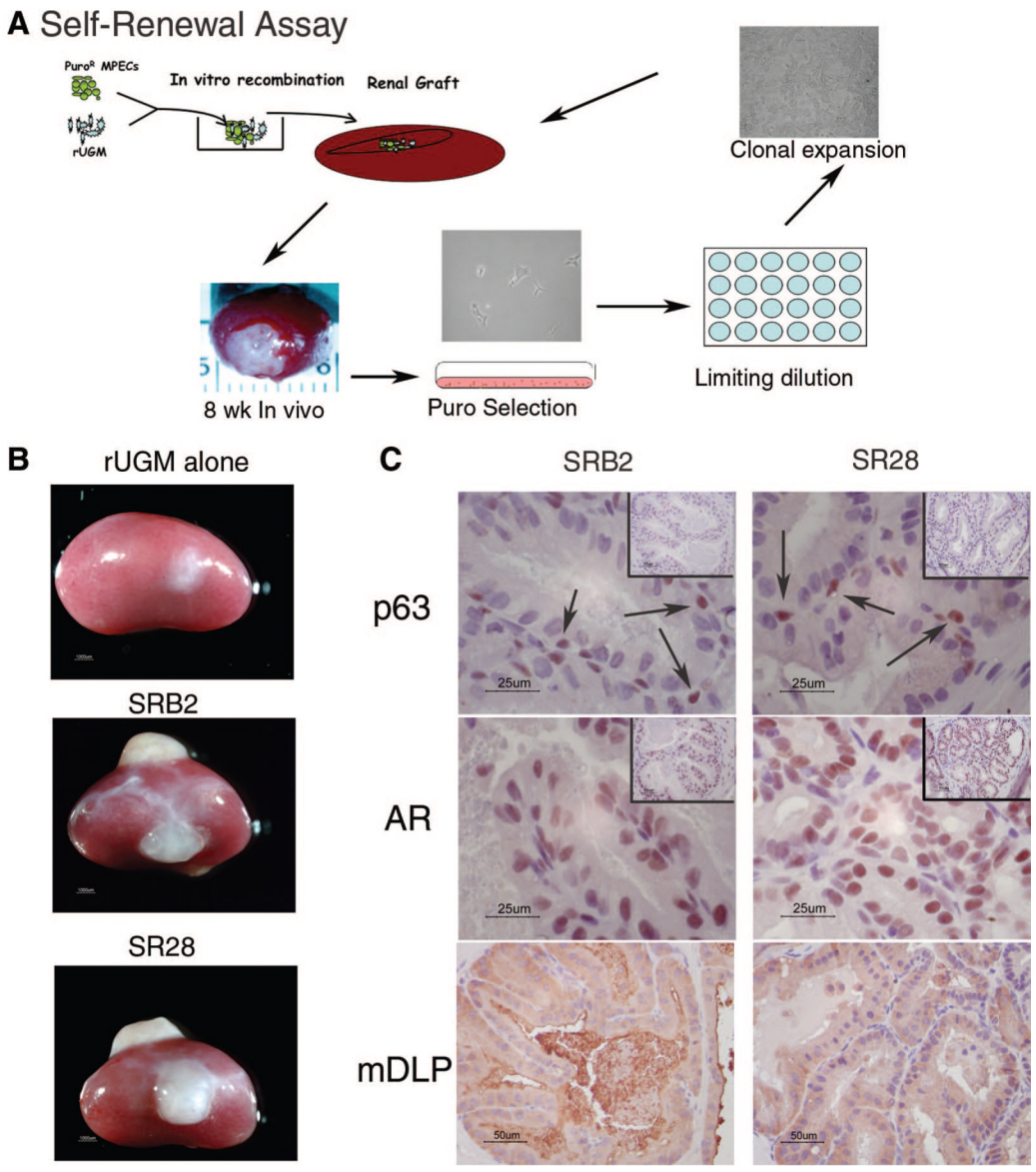

Figure 5.

MPECs retain progenitor/stem cell properties (self-renewal) after serial recombination. **(A):** Schematic of experiment. Clonally derived Puro-resistant MPECs were grafted with urogenital mesenchyme. After 8 wk in vivo, the Puro-resistant cells were rederived by Puro selection. The rederived population was then subjected to limiting dilution and assayed for multilineage differentiation in vivo by reestablishing MPEC/rUGM recombinants under the renal capsules of nude mice. **(B):** Gross pictures of grafts after 10 wk in vivo. **(C):** Immunohistochemical localization of p63, AR, and mDLP. Insets show low magnification of the regions presented at high magnification in the corresponding panels. SRB2 and SR28 are independent clones isolated from separate grafts of WFU3 clone 3 cells as described in Materials and Methods. Abbreviations: AR, androgen receptor; mDLP, mouse dorsolateral secretory protein; MPEC, mouse prostatic epithelial cell; Puro, puromycin; rUGM, rat urogenital mesenchyme; SR, serial recombinant; um, micrometer; wk, weeks.

NIH-PA Author Manuscript
NIH-PA Author Manuscript
NIH-PA Author Manuscript

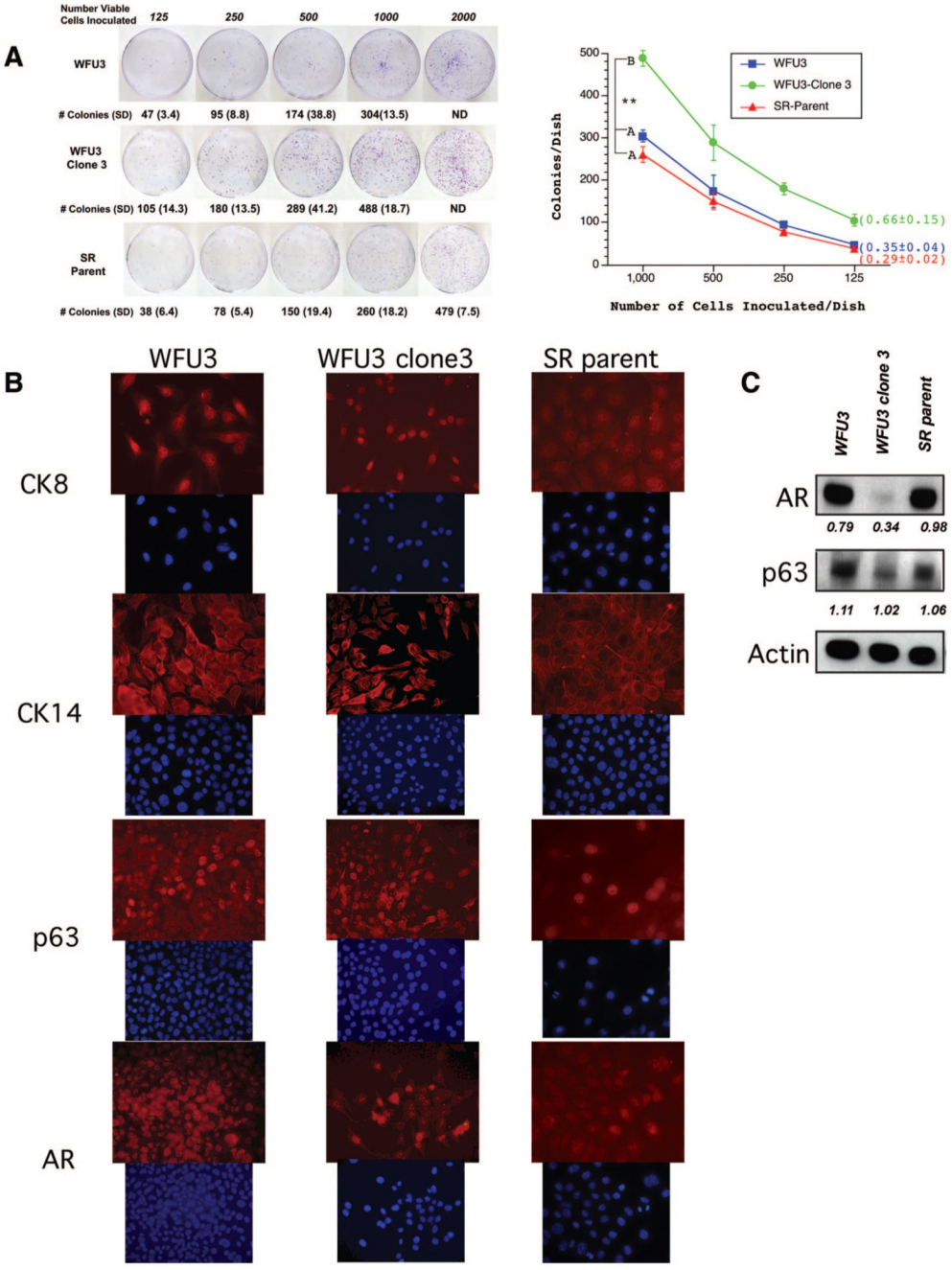

Figure 6.

WFU3 clone 3 cells have enhanced clonogenicity and an increased p63 to AR ratio. **(A):** Clonogenic assays. WFU3, WFU3 clone 3, and SR parent cells were inoculated on 60-mm dishes at the indicated densities and allowed to grow for 4 or 5 days prior to fixation and crystal violet staining as described in Materials and Methods. Left panel shows digital photos of representative dishes after staining. The mean number of colonies ± SD of quadruplicate dishes is depicted below each plate and in the graph at the right. In the graph, lines with the same letter next to them are not statistically significantly different from each other by analysis of variance; $p \leq .05$ was considered significant. **, $p \leq .001$. Numbers in parentheses are the average colony-forming efficiency ± SD of all inoculation densities, excluding 2,000 cells per

dish. (**B)** Immunofluorescence microscopy of monolayer cultures of WFU3, WFU3 clone 3, and SR parent. Each top panel represents detection with a different primary antibody (indicated). Each bottom panel shows detection of 4,6-diamidino-2-phenylindole fluorescence from same area. Original magnification, ×60. **(C):** Immunoblot of protein lysates from the indicated cells probed for AR, p63, and β-actin. The numbers under each lane are the ratio of band intensity relative to actin loading. Abbreviations: AR, androgen receptor; CK, cytokeratin; ND, not determined.

NIH-PA Author Manuscript
NIH-PA Author Manuscript
NIH-PA Author Manuscript

NIH-PA Author Manuscript
NIH-PA Author Manuscript
NIH-PA Author Manuscript

A

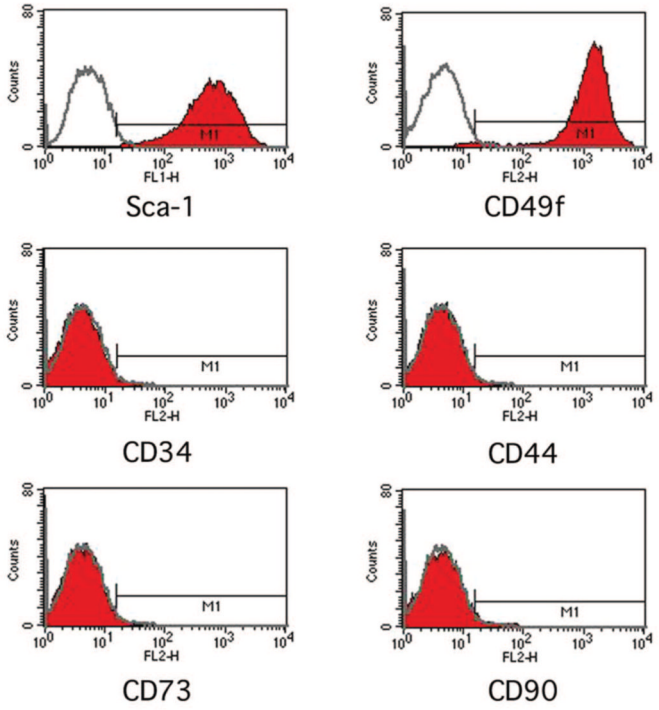

B

		Percent Positive Cells	Median Intensity
Sca-1	**WFU3**	99.1	421.7
	WFU3 clone 3	98.4	544.3
	SR parent	81.5	168.5
CD49F	**WFU3**	98.9	873.8
	WFU3 clone 3	98.8	947.5
	SR parent	99.0	991.1
CD34	**WFU3**	2.1	22.1
	WFU3 clone 3	2.3	19.3
	SR parent	2.5	20.0
CD44	**WFU3**	1.9	21.9
	WFU3 clone 3	2.6	20.5
	SR parent	2.2	19.8
CD73	**WFU3**	2.0	21.3
	WFU3 clone 3	2.1	20.1
	SR parent	2.0	19.9
CD90	**WFU3**	5.7	25.7
	WFU3 clone 3	9.1	24.6
	SR parent	12.1	24.6

Figure 7.

Prostate progenitor/stem cells express stem cell antigen 1 and CD49f. **(A):** Fluorescence-activated cell sorting analysis of WFU3 cells. The gray line in each graph represents the isotype control fluorescence. The solid line with red fill represents the fluorescence with the specific antibody. M1 is the calculated area of positive reactivity based on the isotype control. **(B):** Comparison of cell surface marker expression among WFU3, WFU3 clone 3, and SR parent cells. All cells were grown to 70%-80% confluence, and on the same day, cells were harvested and analyzed for marker expression as described in Materials and Methods.